



# Antimetastatic activity of seongsanamide B in $\gamma$ -irradiated human lung cancer

Ga-Hee Ryoo<sup>a,1</sup>, Geum Jin Kim<sup>b,c,1</sup>, Ah-Reum Han<sup>a</sup>, Chang Hyun Jin<sup>a</sup>, Hunmin Lee<sup>b</sup>, Joo-Won Nam<sup>b</sup>, Hyukjae Choi<sup>b,c,\*\*</sup>, Chan-Hun Jung<sup>d,\*</sup>

<sup>a</sup> Advanced Radiation Technology Institute, Korea Atomic Energy Research Institute, Jeongseup-si, Jeollabuk-do, 56212, South Korea

<sup>b</sup> College of Pharmacy, Yeungnam University, Gyeongsan-si, Gyeongsangbuk-do, 38541, South Korea

<sup>c</sup> Research Institute of Cell Culture, Yeungnam University, Gyeongsan-si, Gyeongsangbuk-do, 38541, South Korea

<sup>d</sup> Jeonju AgroBio-Materials Institute, Jeonju-si, Jeollabuk-do, 54810, South Korea

## ARTICLE INFO

### Keywords:

Lung cancer  
Metastasis  
Seongsanamide B  
Radiation therapy enhancer

## ABSTRACT

Lung cancer, which has a high incidence and mortality rates, often metastasizes and exhibits resistance to radiation therapy. Seongsanamide B has conformational features that suggest it has therapeutic potential; however, its antitumor activity has not yet been reported. We evaluated the possibility of seongsanamide B as a radiation therapy efficiency enhancer to suppress  $\gamma$ -irradiation-induced metastasis in non-small cell lung cancer. Seongsanamide B suppressed non-small cell lung cancer cell migration and invasion caused by  $\gamma$ -irradiation. Furthermore, it suppressed  $\gamma$ -irradiation-induced upregulation of Bcl-X<sub>L</sub> and its downstream signaling molecules, such as superoxide dismutase 2 (SOD2) and phosphorylated Src, by blocking the nuclear translocation of phosphorylated STAT3. Additionally, seongsanamide B markedly modulated the  $\gamma$ -irradiation-induced upregulation of E-cadherin and vimentin. Consistent with the results obtained *in vitro*, while seongsanamide B did not affect xenograft tumor growth, it significantly suppressed  $\gamma$ -irradiation-induced metastasis by inhibiting Bcl-X<sub>L</sub>/SOD2/phosphorylated-Src expression and modulating E-cadherin and vimentin expression in a mouse model. Thus, seongsanamide B may demonstrate potential applicability as a radiation therapy efficiency enhancer for lung cancer treatment.

## 1. Introduction

In 2020, the global mortality rate for newly diagnosed cases of lung cancer was estimated to exceed 80% [1,2]. While the five-year overall survival rate for lung cancer patients has increased due to the early diagnosis of this condition, non-small cell lung cancer (NSCLC), which accounts for approximately 80–90% of cases, is often diagnosed at the advanced stages, making surgical resection difficult [3–5]. Treatment options for NSCLC include chemo-, immune-, radio-, and chemoradiotherapy [5,6]. Although radiation therapy is an effective localized treatment, it can induce radiation-induced metastasis [7]. Therefore, new strategies that combine radiation therapy with enhancers capable of suppressing such metastasis are needed.

\* Corresponding author. JeonJu AgroBio-Materials Institute, Jeonju-si, Jeollabuk-do, 54810, South Korea.

\*\* Corresponding author. College of Pharmacy, Yeungnam University, Gyeongsan-si, Gyeongsangbuk-do, 38541, South Korea.

E-mail addresses: [h5choi@yu.ac.kr](mailto:h5choi@yu.ac.kr) (H. Choi), [chjung@jami.re.kr](mailto:chjung@jami.re.kr), [biohun@gmail.com](mailto:biohun@gmail.com) (C.-H. Jung).

<sup>1</sup> These authors contributed equally.

<https://doi.org/10.1016/j.heliyon.2023.e20179>

Received 1 June 2023; Received in revised form 5 September 2023; Accepted 13 September 2023

Available online 14 September 2023

2405-8440/© 2023 The Authors. Published by Elsevier Ltd. This is an open access article under the CC BY-NC-ND license (<http://creativecommons.org/licenses/by-nc-nd/4.0/>).

## Nomenclature

DPBS	Dulbecco's phosphate-buffered saline
EMT	Epithelial-mesenchymal transition
FBS	Fetal bovine serum
H&E	Hematoxylin and eosin
IL-6	Interleukin-6
IR	Irradiation
NSCLC	Non-small cell lung cancer
SOD2	Superoxide dismutase 2
STAT3	Signal transducer and activator of transcription 3

Signal transducer and activator of transcription 3 (STAT3) plays a critical role in tumorigenesis, including cancer formation, development, and metastasis and is activated in 22%–65% of NSCLCs, with high STAT3 expression indicating a poor prognosis for patients [8–10]. STAT3 is activated through phosphorylation in response to various stimuli, such as interleukin-6 (IL-6), interferon  $\gamma$ , epidermal growth factor, and platelet-derived growth factor, resulting in homodimer formation [11,12]. These activated STAT3 dimers translocate into the nucleus and bind to DNA promoter regions to transcribe genes encoding cell-cycle regulators, such as c-Myc and cyclin D1, and antiapoptotic markers, such as Mcl-1, survivin, Bcl-2, and Bcl-X<sub>L</sub> [13–15]. Constitutively activated STAT3 is closely associated with metastasis in NSCLC patients [16]. Sublethal  $\gamma$ -irradiation can induce tumor invasion, migration, and metastasis via activation of the IL-6/STAT3/Bcl-X<sub>L</sub> signaling pathway [17,18]; exposure to  $\gamma$ -irradiation can also activate epithelial-mesenchymal transition (EMT) progression in lung cancer cells [19]. Therefore, identifying candidates capable of inhibiting IL-6/STAT3/Bcl-X<sub>L</sub> signaling is crucial for developing radiation therapy enhancers that can effectively suppress radiation therapy-induced cancer metastasis.

Seongsanamide B (Fig. 1A) is a bicyclic peptide isolated from *Bacillus safensis* KCTC 12796BP [20]. Its bicyclic structure is considered to confer high conformational rigidity and metabolic stability to the compound [21]. These features are generally associated with high target specificity and resistance to enzymatic digestion, suggesting the high therapeutic potential of the compound [22,23]. Seongsanamides, including seongsanamide B, have been reported to exhibit antiallergic properties in bone marrow-derived mast cells *in vitro* [20]. Furthermore, seongsanamide A exhibited antiallergic activity in a passive cutaneous anaphylaxis mouse model [20]. However, the antitumor effects of seongsanamide B have not yet been reported.

In this study, we evaluated the role of seongsanamide B as a novel radiation therapy enhancer by analyzing its antimetastatic activity in NSCLC cell lines and a metastasis animal model.

## 2. Materials and methods

### 2.1. General experimental procedures

HPLC was performed using the Gilson HPLC system (321 pump and UV/VIS-155 detector) equipped with the Hecor M C18 column (22.5 × 250 mm). Nuclear magnetic resonance spectra were recorded using the AVANCE 400 MHz spectrometer (<sup>1</sup>H, 400 MHz, and <sup>13</sup>C, 100 MHz; Bruker, Billerica, MA, USA) with dimethyl sulfoxide-*d*<sub>6</sub>. Ultraviolet and electronic circular dichroism spectra were obtained using the Cary5000 (Agilent, Santa Clara, CA, USA) and J-810 (Jasco, Tokyo, Japan) spectrophotometers, respectively, at the Research Center for Natural Products and Medical Materials.

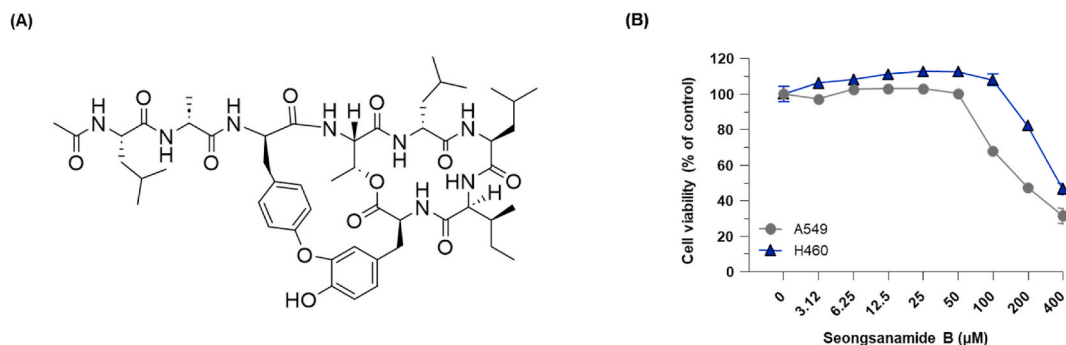


**Fig. 1.** Cytotoxic effect of seongsanamide B on NSCLC cells. (A) Chemical structure of seongsanamide B. (B) Cell viability was measured after treatment with seongsanamide B at various concentrations (3.12, 6.25, 12.5, 2.5, 50, 100, 200, and 400  $\mu$ M) for 48 h. Data are expressed as the mean  $\pm$  standard deviation (SD) (n = 3).

## 2.2. Cell culture and treatments

A549 and H460 NSCLC cells (Korean Cell Line Bank, Seoul, Korea) were cultured in Roswell Park Memorial Institute (RPMI)-1640 medium (Gibco Invitrogen Corp., Grand Island, NY, USA) containing 10% fetal bovine serum (FBS; Gibco Invitrogen Corp.) in a 5% CO<sub>2</sub> atmosphere at 37 °C. For  $\gamma$ -irradiation, A549 and H460 cells were seeded (A549:  $5 \times 10^5$  cells, H460:  $1 \times 10^6$  cells) in a 60-mm<sup>2</sup> culture dish and incubated for 18 h (70–80% confluence). The cells were exposed to  $\gamma$ -irradiation (A549: 10 Gy, H460: 2 Gy) using the <sup>137</sup>Cs  $\gamma$ -ray irradiator (Gammacell 40 Exactor; Nordion International Inc., Ottawa, ON, Canada). After  $\gamma$ -irradiation exposure, the cells were washed with RPMI-1640. Seongsanamide B was isolated from the culture broth of *B. safensis* KCTC 12796BP as described previously [20], and the irradiated cells were treated with seongsanamide B for 24 h or 48 h. After incubation, the cells were harvested for analysis.

## 2.3. Cell viability assay

A549 and H460 cells were seeded in 96-well culture plates (A549:  $1 \times 10^4$  cells/well, H460:  $2 \times 10^4$  cells/well) and treated with seongsanamide B at various concentrations (3.12, 6.25, 12.5, 25, 50, 100, 200, and 400  $\mu$ M) for 48 h. Then, 10  $\mu$ L of EZ-Cyto cell viability assay reagent (DoGenBio, Seoul, Korea) was added to each well, and the plate was incubated for 4 h. Then, the absorbance at a 450 nm wavelength was determined using the Multiskan SkyHigh Microplate Spectrophotometer (Thermo Fisher Scientific, Waltham, MA, USA) to determine the effect of seongsanamide B on cell viability.

## 2.4. Wound healing assay

To assess the effect of seongsanamide B on IR-induced migration, cells were seeded in 6-well culture plates (A549:  $2.5 \times 10^5$  cells/well, H460:  $5 \times 10^5$  cells/well) and incubated for 24 h. Scrapes of similar thickness were made on the cell layer. The cells were exposed to  $\gamma$ -irradiation (A549: 10 Gy, H460: 2 Gy), 50  $\mu$ M seongsanamide B was administered, and the cells were incubated for 48 h. Images of the wounds were captured at 0 h and 48 h using the CKX31 microscope (Olympus, Tokyo, Japan) connected to the Moticam 3+ camera (Motic, Kowloon, Hong Kong). The relative wound width was calculated using the following formula: wound width (%) = (wound width after 48 h/initial wound width)  $\times$  100.

## 2.5. Invasion assay

$\gamma$ -Irradiated NSCLC cells (A549: 10 Gy, H460: 2 Gy) were seeded (A549:  $1 \times 10^4$  cells, H460:  $2 \times 10^4$  cells/well) into Matrigel-coated 6.5-mm Transwell inserts (Corning, Glendale, AZ, USA) in serum-free RPMI-1640, and seongsanamide B was added. The inserts were placed in a 24-well culture plate, and the wells were filled with RPMI-1640 containing 10% FBS. After 16 h, invaded cells were fixed with 3.8% formaldehyde (Sigma-Aldrich, St. Louis, MO, USA) for 10 min and stained with 0.23% crystal violet (Sigma-Aldrich) for 30 min. Invaded cells were imaged and counted under a CKX31 microscope.

## 2.6. Nuclear fractionation

Nuclear fractionation was carried out using the NE-PER Nuclear and Cytoplasmic Extraction Reagent kit (Thermo Fisher Scientific). Briefly, harvested cells were washed with PBS (Thermo Fisher Scientific) and suspended in ice-cold CER I containing a protease inhibitor cocktail (Sigma-Aldrich). After 10 min on ice, ice-cold CER II was added. The lysate was separated from the supernatant and pelleted using centrifugation (4 °C, 5 min,  $\sim 16,000\times g$ ). The pellet was suspended in ice-cold NER for 40 min using a vortex mixer, and the nuclear extract (supernatant) was isolated using centrifugation (4 °C, 10 min,  $\sim 16,000\times g$ ).

## 2.7. Enzyme-linked immunosorbent assay

IL-6 protein levels in the medium were measured using the Quantikine ELISA kit (R&D systems, Minneapolis, MN, USA) according to the manufacturer's instructions.

## 2.8. Western blotting

NSCLC cell lysates and mouse lung tissue were prepared using a cell lysis buffer and T-PER™ Tissue Protein Extraction Reagent Kit (Thermo Fisher Scientific) containing a protease and phosphatase inhibitor cocktail (Sigma-Aldrich). Equal amounts of cell lysates (15  $\mu$ g) were separated using sodium dodecyl-sulfate polyacrylamide gel electrophoresis and transferred to polyvinylidene difluoride membranes (Thermo Fisher Scientific). The membranes blocked with 5% skim milk were probed with primary antibodies against  $\beta$ -catenin (#8480), p-STAT3 (#9145), STAT3 (#9139), Bcl-X<sub>L</sub> (#2762), p-Src (#12432), Src (#2109), SOD2 (#13141), E-cadherin (#14472), vimentin (#5741) (Cell Signaling Technology, Danvers, MA, USA), and  $\beta$ -actin (#A5441; Sigma-Aldrich) overnight. Following three washes with a buffer (0.05% Tween in PBS), the membranes were probed with horseradish peroxidase-conjugated secondary antibodies (Thermo Fisher Scientific) at room temperature for 1 h. Antibody signals were detected using the iBright 1500 Imaging System (Invitrogen, Waltham, MA, USA).

## 2.9. Animal studies

BALB/c mice (5–6-week-old females; Orient Bio Inc., Gyeonggi-do, Korea) were acclimated for a week in a climate-controlled room ( $22 \pm 2^\circ\text{C}$ ,  $55\% \pm 5\%$  relative humidity, 12 h light/dark cycle). All animal care and ethics protocols and experiments were approved by the Institutional Animal Care and Use Committee of Jeonbuk National University Hospital (approval numbers JBUH-IACUC-2020-7 and JBUH-IACUC-2021-10-1, Jeonju, Korea).

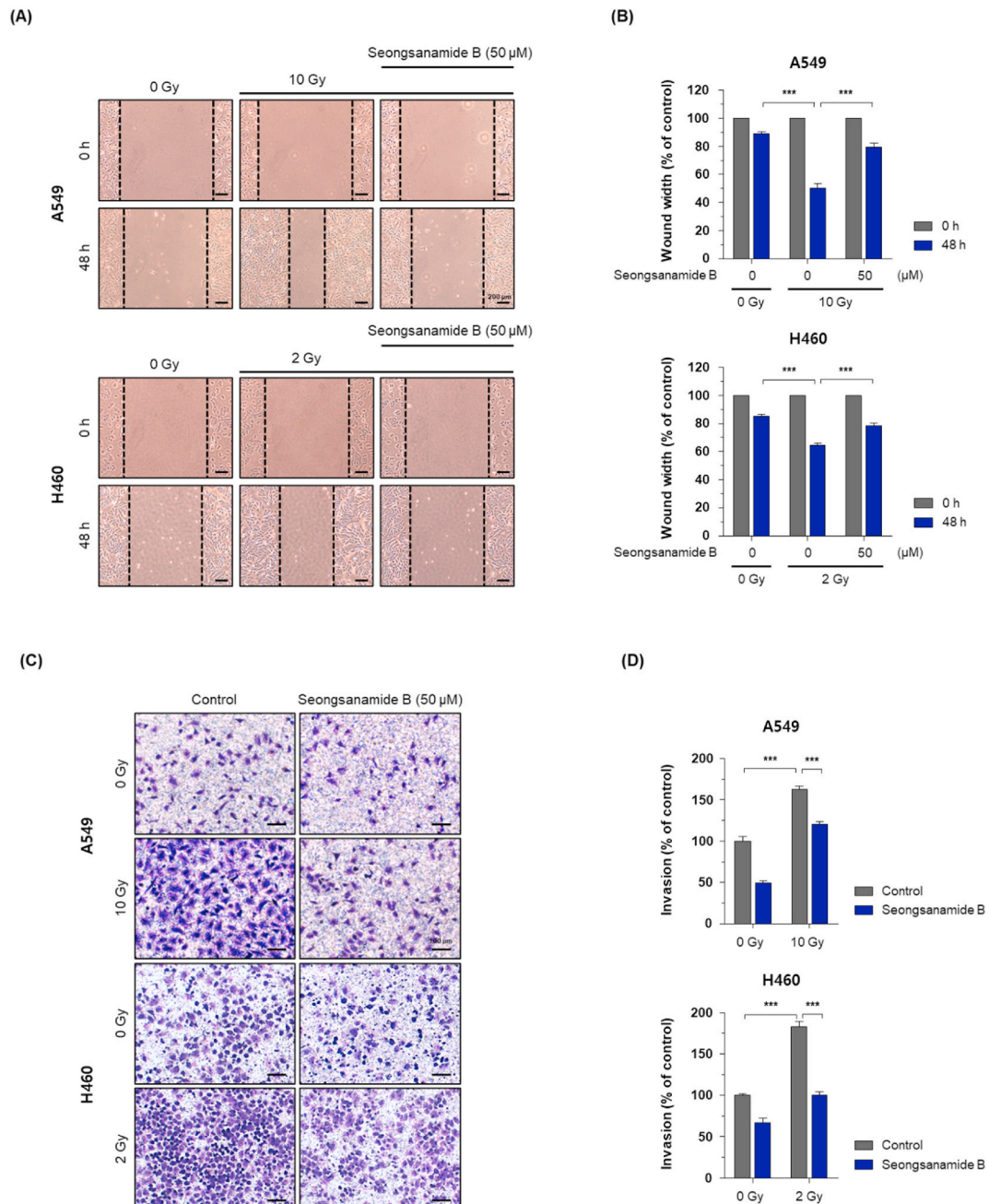


**Fig. 2.** Seongsanamide B suppresses IR-induced cancer cell migration and invasion. (A) A wound healing assay was performed to determine the inhibitory effect of seongsanamide B on IR-induced enhancement of the migration abilities of A549 and H460 cells. Quantitative data are shown in (B). (C) An invasion assay was used to determine the inhibitory effect of seongsanamide B on the IR-induced enhancement of the invasion abilities of A549 and H460 cells. Quantitative data are shown in (D). Data are expressed as the mean  $\pm$  SD ( $n = 3$ ). \*\*\* $p < 0.001$ .

## 2.10. Xenograft tumor

A549 cells were mixed with Matrigel at a 1:1 ratio. The cells were subcutaneously injected into the flanks of mice ( $1 \times 10^6$  cells, 100  $\mu$ L). When the xenograft tumors reached 100–200 mm<sup>3</sup>, the mice were divided into four treatment groups (control and 1, 2.5, or 5 mg/kg of seongsanamide B; n = 4 in each group). Seongsanamide B or DPBS (Thermo Fisher Scientific) was intraperitoneally administered daily for 14 days. Tumor volumes ( $(\text{width}^2 \times \text{length})/2$ ) were determined using a caliper twice a week for 27 days.

## 2.11. Analysis of $\gamma$ -irradiation-Induced metastasis in an animal model

A549 cells were cultured in a 100-mm<sup>2</sup> dish until they reached 70–80% confluence and exposed to 2 Gy of  $\gamma$ -irradiation using a TrueBeam instrument (Varian Medical Systems, Palo Alto, CA, USA). BALB/c mice (6 weeks old) were divided into four groups (0 Gy/DPBS, n = 5; 0 Gy/5 mg/kg of seongsanamide B, n = 7; 2 Gy/DPBS, n = 5; 2 Gy/5 mg/kg of seongsanamide B, n = 7), and  $\gamma$ -irradiated A549 cells were injected in all mice via the tail vein. Seongsanamide B or DPBS was intraperitoneally administered daily for 7 weeks. Their body weight was measured once a week for 7 weeks. After euthanizing the mice with ketamine, their lungs were collected. Images of lung tissues were captured, and the metastatic lung nodules were counted. Histological and Western blot analyses were performed on the lung tissues.

## 2.12. Histological analysis

Lung tissues were fixed with 10% formalin and embedded in paraffin. After staining with hematoxylin and eosin (H&E), the metastatic lung nodules were imaged and analyzed using the Motic EasyScan One Digital Slide Scanner (Motic, Kowloon, Hong Kong).

## 2.13. Statistical analysis

The results are expressed as the mean  $\pm$  SD of three independent experiments. Statistical significance was considered as  $p < 0.05$ , which was statistically analyzed using Student's *t*-test or one-way ANOVA with Tukey post-hoc comparison on GraphPad Prism Software (GraphPad Software, San Diego, CA, USA).

# 3. Results

## 3.1. Seongsanamide B exerts a cytotoxic effect on NSCLC cells

In our previous screening of new bioactive natural products from marine-derived microbes, seongsanamide B was identified in *Bacillus safensis* KCTC 12796BP culture broth as a bicyclic peptide in the class of seongsanamides, which are biosynthesized by a non-ribosomal peptide synthetase (Fig. 1A) [20,24]. We evaluated the cytotoxic effect of seongsanamide B in NSCLC cell lines (A549 and H460) to investigate its possibility as a radiation therapy enhancer for radiation combination therapy in lung cancer. The cytotoxic effect of seongsanamide B at various concentrations (3.12, 6.25, 12.5, 25, 50, 100, 200, and 400  $\mu$ M) was measured in cells treated with the compound for 48 h. The half-maximal inhibitory concentration of seongsanamide B in A549 and H460 cells was 204.4  $\mu$ M and 376.7  $\mu$ M, respectively (Fig. 1B). These results indicate that seongsanamide B showed no cytotoxic effects at concentrations below 50  $\mu$ M in A549 and H460 cells.

## 3.2. Seongsanamide B suppresses NSCLC cell migration and invasion induced by $\gamma$ -radiation

To investigate the anti-migration effect of seongsanamide B in cells exposed to IR, wound healing assay was performed. The scratch wound width of A549 and H460 cells rapidly recovered after 10 Gy and 2 Gy of IR exposure (Fig. 2A). The rapid recovery caused by IR exposure was significantly suppressed after treatment with 50  $\mu$ M seongsanamide B in both A549 and H460 cells (Fig. 2B). Furthermore, we performed cell viability assay to confirm whether IR could affect the anti-migration effect of seongsanamide B. As shown in Fig. S1, IR (10 Gy and 2 Gy) did not affect the cell viability in A549 and H460 cells, respectively. This result indicates that seongsanamide B suppresses the IR-induced enhancement of tumor cell migration.

Next, we performed invasion assays to evaluate whether seongsanamide B could also inhibit the IR-induced enhancement of the invasion ability of tumor cells. As expected, IR (10 Gy and 2 Gy) promoted the invasion abilities of A549 and H460 cells; 50  $\mu$ M seongsanamide B treatment suppressed these effects (Fig. 2C and D). This indicates that seongsanamide B suppresses IR-induced enhancement of cell invasion abilities. These results indicate that seongsanamide B suppresses the IR exposure-induced enhancement of the migration and invasion abilities of A549 and H460 lung cancer cells.

## 3.3. Seongsanamide B suppresses IR-induced enhancement of the migration and invasion abilities of cancer cells by blocking p-STAT3 translocation

We previously demonstrated that IR exposure induces malignant effects, such as enhanced migration and invasion abilities, via signaling pathways involving  $\beta$ -catenin, IL-6, STAT3, Bcl-X<sub>L</sub>, superoxide dismutase 2 (SOD2), and Src [17–19]. Therefore, we analyzed IR-induced signaling molecules using an ELISA kit and western blotting to investigate the mechanism of seongsanamide B in inhibiting

cell migration and invasion induced by IR in NSCLC cells. First, we measured the expression of rH2AX to validate the accuracy of irradiation dosage. As shown in Fig. S2, we confirmed that the expression of rH2AX is induced after exposing 10 Gy or 2 Gy IR in A549 and H460 cells, respectively. IR (10 Gy and 2 Gy) sequentially activated  $\beta$ -catenin, IL-6, p-STAT3, Src, Bcl-X<sub>L</sub>, and SOD2 in A549 and H460 cells (Fig. 3A and B). Treatment with 50  $\mu$ M seongsanamide B reduced IR-induced Bcl-X<sub>L</sub>, SOD2, and p-Src expression but did not decrease the expression of upstream signaling molecules, including  $\beta$ -catenin, IL-6, and phosphorylated STAT3 in A549 and H460 cells. Activated STAT3 with tyrosine phosphorylation translocates into the nucleus to activate various genes, including Bcl-X<sub>L</sub> [25], and seongsanamide B inhibited IR-induced STAT3-Bcl-X<sub>L</sub> signaling in this study. Therefore, to investigate whether seongsanamide B reduced Bcl-X<sub>L</sub> expression by blocking activated STAT3 translocation, we determined the phosphorylated STAT3 level in cells subjected to nuclear fractionation using western blotting. As shown in Fig. 3C, IR (10 Gy and 2 Gy) increased the level of p-STAT3 in the nuclear fraction, and p-STAT3 translocation was inhibited after 50  $\mu$ M seongsanamide B treatment. These results suggest that seongsanamide B may suppress IR-induced cell migration and invasion by blocking p-STAT3 nuclear translocation in NSCLC cells.

### 3.4. Seongsanamide B suppresses IR-induced EMT

The EMT process is activated by various intrinsic and extrinsic signaling factors, including STAT3, which regulate migration and invasion [26,27]. IR induces cell migration and invasion by regulating STAT3 phosphorylation in various cancer cells. Furthermore, IR promotes EMT via the Src-mediated signaling pathway [28]. Therefore, to evaluate the effects of seongsanamide B on IR-induced EMT in NSCLC cells, using western blotting, we analyzed the levels of the EMT markers E-cadherin and vimentin after exposure to IR. The E-cadherin levels decreased, whereas vimentin levels increased in A549 and H460 cells after exposure to 10 Gy and 2 Gy IR (Fig. 4). These changes were recovered after treatment with 50  $\mu$ M seongsanamide B. This suggests that seongsanamide B suppresses IR-induced EMT in NSCLC cells.

### 3.5. Seongsanamide B attenuates IR-induced metastasis in animal model

In the present study, seongsanamide B showed inhibitory activities against IR-induced cell migration and invasion. Therefore, we evaluated the inhibitory effect of seongsanamide B on IR-induced metastasis *in vivo* to develop a radiation therapy enhancer. We first investigated the cytotoxicity of seongsanamide B to find a non-toxic concentration *in vivo* using a xenograft model (Fig. 5A–C). The xenograft tumor study was performed with DPBS or seongsanamide B (1, 2.5, or 5 mg/kg) as shown in Fig. 5A. No significant differences in body weight were observed among the four treatment groups (control and 1, 2.5, and 5 mg/kg seongsanamide B) (Fig. 5B). Xenograft tumor growth was not significantly affected by seongsanamide B treatment (Fig. 5C). This suggests that seongsanamide B, at a concentration of up to 5 mg/kg, does not affect xenograft tumor growth.

We then performed metastasis animal study using the IR-induced metastasis model established in a previous study [29] to investigate whether seongsanamide B suppressed IR-induced metastasis *in vivo* (Fig. 5D). No significant differences in body weight were observed among the four groups (0 Gy/DPBS, 0 Gy/seongsanamide B [5 mg/kg], 2 Gy/DPBS, 2 Gy/seongsanamide B [5 mg/kg]) (Fig. 5E). The number of metastatic lung nodules was significantly enhanced after 2 Gy IR exposure, and this effect was significantly

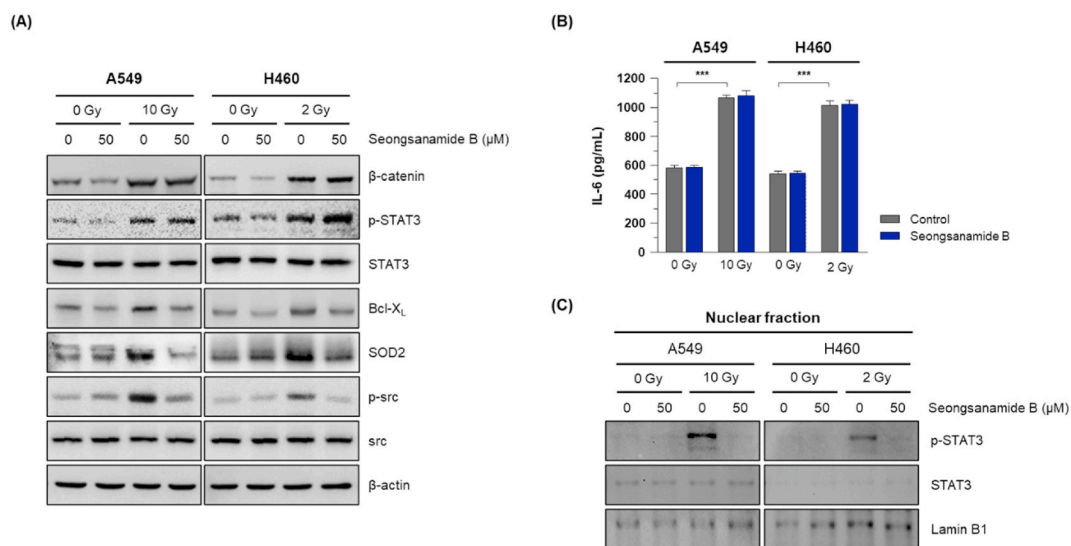


**Fig. 3.** Seongsanamide B suppresses IR-induced cell migration and invasion by blocking STAT3 phosphorylation. Irradiated (A549; 10 Gy, H460; 2 Gy) and untreated control A549 and H460 cells were treated with 50  $\mu$ M seongsanamide B or left untreated, and protein levels were measured using western blotting (A) and an ELISA kit (B). Data are expressed as the mean  $\pm$  SD (n = 6). \*\*\**p* < 0.001. (C) Nuclear fractions were prepared using a cell fractionation kit, and STAT3 and p-STAT3 levels were measured using western blotting. Lamin B1 was used as a loading control. The uncropped images of western blotting were referred in Supplemental Material.

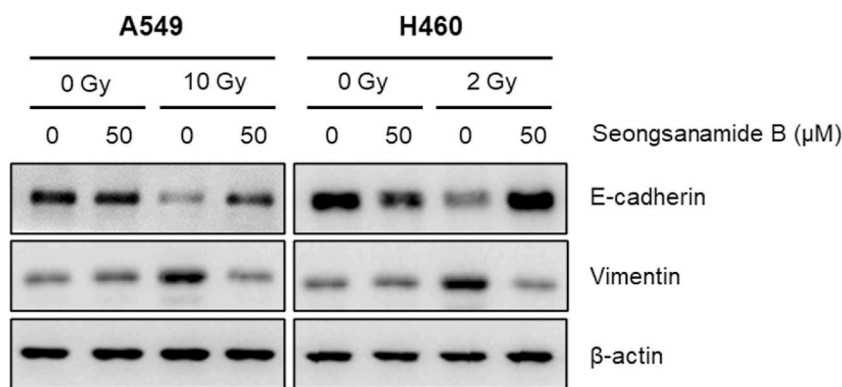


**Fig. 4.** Seongsanamide B suppresses IR-induced EMT. Irradiated (A549; 10 Gy, H460; 2 Gy) and untreated control A549 and H460 cells were treated with 50  $\mu$ M seongsanamide or left untreated; E-cadherin and vimentin protein levels were measured using western blotting. The uncropped images of western blotting were referred in Supplemental Material.

suppressed by 5 mg/kg seongsanamide B treatment (Fig. 5F). To confirm these effects, we histologically analyzed the cells using H&E staining (Fig. 5G). Next, we analyzed the expression of IR-induced signaling molecules to investigate the mechanism whereby seongsanamide B inhibits IR-induced metastasis *in vivo* using western blotting. The protein levels of p-STAT3, Bcl-X<sub>L</sub> and Src signaling molecules increased after 2 Gy IR exposure, consequently inducing EMT, in line with the *in vitro* experimental results (Figs. S3 and 5H). These effects were significantly suppressed by seongsanamide B treatment. These results suggest that seongsanamide B suppresses IR-induced metastasis *in vivo* by suppressing EMT via the Bcl-X<sub>L</sub> and Src signaling pathways.

#### 4. Discussion

Radiation therapy using ionizing radiation is a major therapeutic modality for treating cancer [5,6]. In NSCLC patients, radiation therapy is effective for localized application but often causes IR-induced metastasis [7]. Sublethal doses of IR promote tumor invasion, migration, and metastasis *in vitro* and *in vivo*, mediated by the IR-induced IL-6/STAT3/Bcl-X<sub>L</sub> signaling pathway, which is a potential therapeutic target for developing radiation therapy enhancers [17,18,30,31]. We continue to search for radiation therapy enhancers that effectively suppress IR-induced malignant effects. In a previous study, seongsanamide B, a bicyclic peptide in the class of seongsanamides biosynthesized by a non-ribosomal peptide synthetase, was isolated from marine-derived microbes [20]. The bicyclic peptide has isodityrosine residue, which is a tyrosine dimer linked through a diaryl ether moiety [32]. The diaryl ether is functional scaffold that are considered fundamental fragment of a variety of medicinal drugs as well as their bioisosteres [33,34]. Due to the potential structural diversity of seongsanamides, it is thought that it will be applied to various drugs, but its bioactive properties have not yet been well studied [21].

In this study, we investigated the potential of seongsanamide B to serve as a radiation therapy enhancer to prevent IR-induced metastasis in NSCLC. As we aimed to search for candidate radiation therapy enhancers to inhibit IR-induced metastasis without exerting toxic effects on cells. We first determined that 50  $\mu$ M of seongsanamide B is the non-toxic concentration in NSCLC cell lines. Next, we showed that seongsanamide B suppresses the IR exposure-induced enhancement of the migration and invasion abilities of A549 and H460 lung cancer cells. IR promotes migration and invasion through various signaling pathways, including those involving  $\beta$ -catenin, IL-6, STAT3, Bcl-X<sub>L</sub>, SOD2, and Src, all of which are associated with malignancy [17–19]. Among them, STAT3 is an important target for radiation therapy enhancers because STAT3 is closely linked to various malignant effects, including proliferation, survival, tumorigenesis, angiogenesis, metastasis, and EMT [11,12,27,35]. In response to IR, activated STAT3 with tyrosine phosphorylation translocates into the nucleus to activate various genes; this induces cancer cell migration, invasion, and metastasis [36]. We observed that seongsanamide B inhibited IR-induced upregulation of Bcl-X<sub>L</sub>, SOD2, and p-Src expression by blocking the nuclear translocation of phosphorylated STAT3. This result suggests that seongsanamide B suppresses IR-induced cell migration and invasion in NSCLC cells by blocking nuclear translocation of phosphorylated STAT3. Furthermore, we showed that seongsanamide B suppresses IR-induced EMT in NSCLC cells. To confirm the potential of seongsanamide B as a radiation therapy enhancer *in vivo*, we evaluated its antimetastatic activity using an IR-induced metastasis animal model established in a previous study. We observed that seongsanamide B had no effect on xenograft tumor growth at concentration up to 5 mg/kg. For that reason, we chose seongsanamide B at a dose of 5 mg/kg to further evaluate its potential as a radiation therapy enhancer under non-toxic conditions.

In conclusion, seongsanamide B showed potential radiation therapy-enhancing activity in NSCLC cells. Seongsanamide B inhibited IR-induced malignant effects, such as migration and invasion by suppressing Bcl-X<sub>L</sub>/SOD2/p-Src expression and regulating EMT marker expression in NSCLC cells. In addition, seongsanamide B inhibited IR-induced metastasis by suppressing Bcl-X<sub>L</sub>/SOD2/p-Src expression and modulating EMT markers, E-cadherin and vimentin, in animal study. These our results suggest that seongsanamide B has potential as a radiation therapy enhancer to suppress IR-induced metastasis *in vivo* via the Src signaling pathways. Although the use of seongsanamide B as a radiation therapy enhancer requires further studies on its safety and effectiveness, seongsanamide B shows promise as a novel radiation therapy enhancer candidate to overcome IR-induced metastatic activity in NSCLC

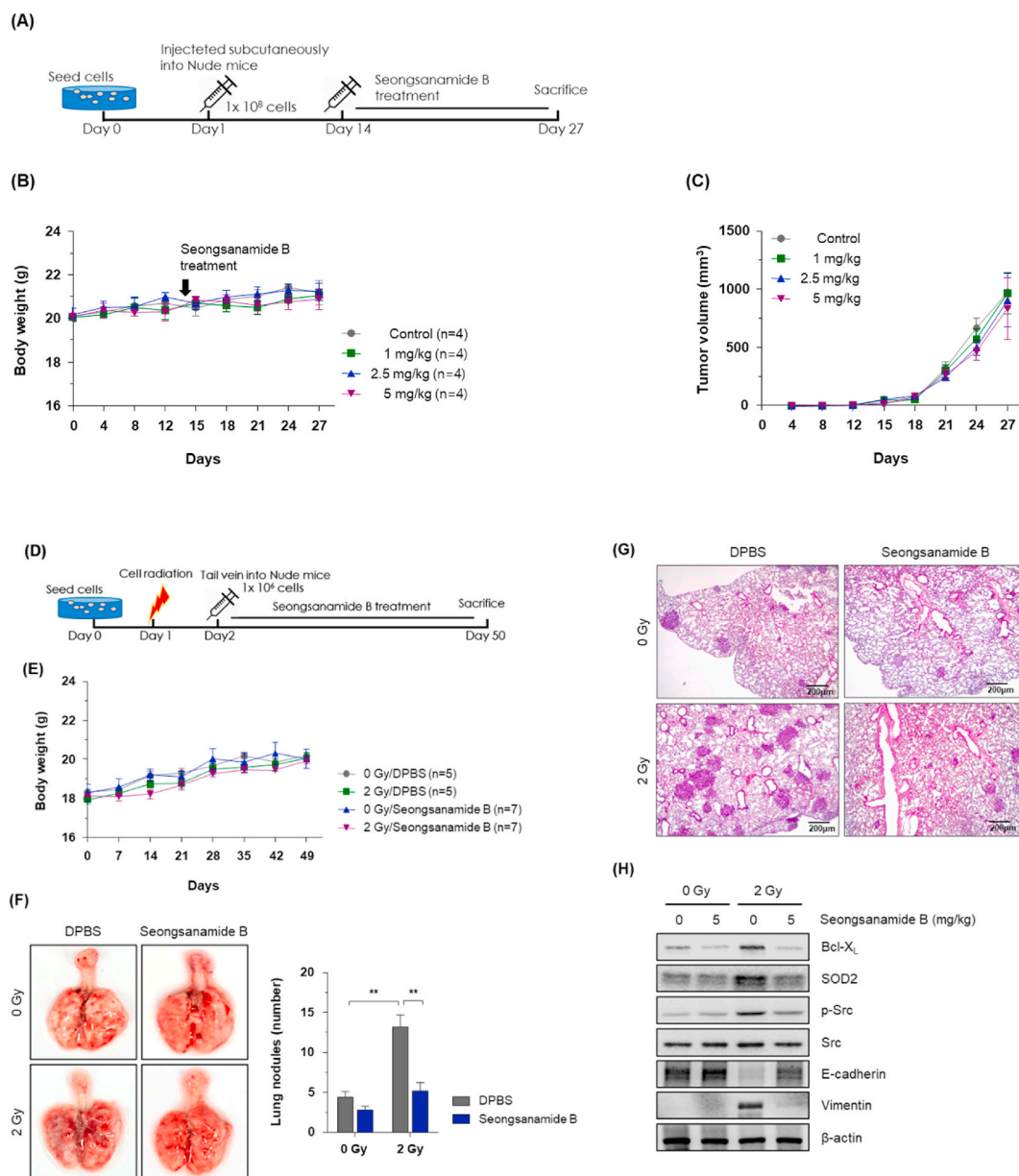


**Fig. 5.** Antimetastatic effects of seongsanamide B in an animal model. (A) Schematic diagram of the xenograft tumor experiment. (B) Body weights in the xenografted and control mice. (C) Tumor volumes in the xenografted and control mice. (D) Schematic diagram of the IR-induced metastasis experiment. (E) Body weights in the metastatic model and control mice. (F) Changes in metastatic lung nodules. Representative lung images. Data are expressed as the mean  $\pm$  SD ( $n = 3$ ). \*\* $p < 0.005$  (G) H&E staining of lung tissues. Scale bar; 200  $\mu$ m. (H) Western blotting analyses of Bcl-X<sub>L</sub>, SOD2, p-Src, Src, E-cadherin, and vimentin levels in lung tissues. The uncropped images of western blotting were referred in Supplemental Material.

patients.

#### Author contribution statement

Ga-Hee Ryoo: Geum Jin Kim: Performed the experiments; Analyzed and interpreted the data; Contributed reagents, materials, analysis tools or data.

Ah-Reum Han: Hyukjae Choi: Conceived and designed the experiments; Wrote the paper.

Chang Hyun Jin: Joo-Won Nam: Contributed reagents, materials, analysis tools or data.

Hunmin Lee: Performed the experiments.

Chan-Hun Jung: Conceived and designed the experiments; Analyzed and interpreted the data; Wrote the paper.

## Data availability statement

Data will be made available on request.

## Declaration of competing interest

The authors declare that they have no known competing financial interests or personal relationships that could have appeared to influence the work reported in this paper.

## Acknowledgements

This research was supported by the National Research Foundation of Korea (NRF) grant funded by the Korean government (Ministry of Science and ICT) (2021R1F1A1060363, NRF-2021R1A2C1010727 and NRF-2020R1A6A1A03044512) and the research program of Korea Atomic Energy Research Institute (Project No. 523310-22). The authors thank the Research Center for Natural Products and Medical Materials (RCNM) for technical support regarding the ECD spectrometer.

## Appendix A. Supplementary data

Supplementary data to this article can be found online at <https://doi.org/10.1016/j.heliyon.2023.e20179>.

## References

- [1] M.G. Raso, N. Bota-Rabasedas, I.I. Wistuba, Pathology and classification of SCLC, *Cancers* 13 (4) (2021) 820.
- [2] R.L. Siegel, K.D. Miller, H.E. Fuchs, A. Jemal, Cancer statistics, 2021, *CA Cancer J. Clin.* 71 (1) (2021) 7–33.
- [3] H. Sung, J. Ferlay, R.L. Siegel, M. Laversanne, I. Soerjomataram, A. Jemal, F. Bray, Global cancer statistics 2020: GLOBOCAN estimates of incidence and mortality worldwide for 36 cancers in 185 countries, *CA Cancer J. Clin.* 71 (3) (2021) 209–249.
- [4] R. Nooreldeen, H. Bach, Current and future development in lung cancer diagnosis, *Int. J. Mol. Sci.* 22 (16) (2021) 8661.
- [5] N. Duma, R. Santana-Davila, J.R. Molina, Non-small cell lung cancer: epidemiology, screening, diagnosis, and treatment, *Mayo Clin. Proc.* 94 (8) (2019) 1623–1640.
- [6] S. Heynemann, P. Mitchell, Developments in systemic therapies for the management of lung cancer, *Intern. Med. J.* 51 (12) (2021) 2012–2020.
- [7] M. Vilalta, M. Rafat, E.E. Graves, Effects of radiation on metastasis and tumor cell migration, *Cell. Mol. Life Sci.* 73 (2016) 2999–3007.
- [8] H.Q. Wang, Q.W. Man, F.Y. Huo, X. Gao, H. Lin, S.R. Li, J. Wang, F.C. Su, L. Cai, Y. Shi, B. Liu, L.L. Bu, STAT3 pathway in cancers: past, present, and future, *MedComm* 3 (2) (2022) e124.
- [9] X. Wang, P.J. Crowe, D. Goldstein, J.L. Yang, STAT3 inhibition, a novel approach to enhancing targeted therapy in human cancers (review), *Int. J. Oncol.* 41 (4) (2012) 1181–1191.
- [10] Y.H. Xu, S. Lu, A meta-analysis of STAT3 and phospho-STAT3 expression and survival of patients with non-small-cell lung cancer, *Eur. J. Surg. Oncol.* 40 (3) (2014) 311–317.
- [11] Z. Zhong, Z. Wen, J.E. Darnell Jr., Stat3: a STAT family member activated by tyrosine phosphorylation in response to epidermal growth factor and interleukin-6, *Science* 264 (5155) (1994) 95–98.
- [12] A. Xiong, Z. Yang, Y. Shen, J. Zhou, Q. Shen, Transcription factor STAT3 as a novel molecular target for cancer prevention, *Cancers* 6 (2) (2014) 926–957.
- [13] M. Snyder, X.Y. Huang, J.J. Zhang, Identification of novel direct Stat3 target genes for control of growth and differentiation, *J. Biol. Chem.* 283 (7) (2008) 3791–3798.
- [14] R.L. Carpenter, H.W. Lo, STAT3 target genes relevant to human cancers, *Cancers* 6 (2) (2014) 897–925.
- [15] L. Zhuang, C.S. Lee, R.A. Scolyer, S.W. McCarthy, X.D. Zhang, J.F. Thompson, P. Hersey, Mcl-1, bcl-XL and Stat3 expression are associated with progression of melanoma whereas bcl-2, AP-2 and MITF levels decrease during progression of melanoma, *Mod. Pathol.* 20 (4) (2007) 416–426.
- [16] S. Parakh, M. Ernst, A.R. Poh, Multicellular effects of STAT3 in non-small cell lung cancer: mechanistic insights and therapeutic opportunities, *Cancers* 13 (24) (2021) 6228.
- [17] C.H. Jung, J.N. Ho, J.K. Park, E.M. Kim, S.G. Hwang, H.D. Um, Involvement of SULF2 in  $\gamma$ -irradiation-induced invasion and resistance of cancer cells by inducing IL-6 expression, *Oncotarget* 7 (2016) 16090–16103.
- [18] C.H. Jung, E.M. Kim, J.Y. Song, J.K. Park, H.D. Um, Mitochondrial superoxide dismutase 2 mediates  $\gamma$ -irradiation-induced cancer cell invasion, *Exp. Mol. Med.* 51 (2019) 1–10.
- [19] E.M. Kim, C.H. Jung, J.Y. Song, J.K. Park, H.D. Um, Pro-apoptotic bax promotes mesenchymal-epithelial transition by binding to respiratory complex-I and antagonizing the malignant actions of pro-survival bcl-2 proteins, *Cancer Lett.* 424 (28) (2018) 127–135.
- [20] G.J. Kim, X. Li, S.H. Kim, I. Yang, D. Hahn, J. Chin, S.J. Nam, J.W. Nam, D.H. Nam, D.C. Oh, H.W. Chang, H. Choi, A.-D. Seongsanamides, Antiallergic bicyclic peptides from *Bacillus safensis* KCTC 12796 BP, *Org. Lett.* 20 (23) (2018) 7539–7543.
- [21] Z. Wu, G.J. Kim, S.Y. Park, J.C. Shon, K.H. Liu, H. Choi, In vitro metabolism study of seongsanamide A in human liver microsomes using non-targeted metabolomics and feature-based molecular networking, *Pharmaceutics* 13 (7) (2021) 1031.
- [22] C.A. Rhodes, D. Pei, Bicyclic peptides as next-generation therapeutics, *Chemistry* 23 (52) (2017) 12690–12703.
- [23] A. Zorzi, K. Deyle, C. Heinis, Cyclic peptide therapeutics: past, present and future, *Curr. Opin. Chem. Biol.* 38 (2017) 24–29.
- [24] S. Shabani, C.A. Hutton, Total synthesis of seongsanamide B, *Org. Lett.* 22 (11) (2020) 4557–4561.
- [25] W.H. Lin, Y.W. Chang, M.X. Hong, T.C. Hsu, K.C. Lee, C. Lin, J.L. Lee, STAT3 phosphorylation at Ser727 and Tyr705 differentially regulates the EMT-MET switch and cancer metastasis, *Oncogene* 40 (2021) 791–805.
- [26] X. Liu, F. Yun, L. Shi, X.H. Li, N.R. Luo, Y.F. Jia, Roles of signaling pathways in the epithelial-mesenchymal transition in cancer, *Asian Pac. J. Cancer Prev.* 16 (15) (2015) 6201–6206.
- [27] Y. Teng, J.L. Ross, J.K. Cowell, The involvement of JAK-STAT3 in cell motility, invasion, and metastasis, *JAK-STAT* 3 (2014), e28086.
- [28] R.K. Kim, Y.H. Cui, K.C. Yoo, I.G. Kim, M. Lee, Y.H. Choi, Y. Suh, S.J. Lee, Radiation promotes malignant phenotypes through SRC in breast cancer cells, *Cancer Sci.* 106 (1) (2015) 78–85.
- [29] Y.R. Kim, A.R. Han, J.B. Kim, C.H. Jung, Dendrobine inhibits  $\gamma$ -irradiation-induced cancer cell migration, invasion and metastasis in non-small cell lung cancer cells, *Biomedicine* 9 (8) (2021) 954.
- [30] M. Fujita, S. Yamada, T. Imai, Irradiation induces diverse changes in invasive potential in cancer cell lines, *Semin. Cancer Biol.* 35 (2015) 45–52.

- [31] K. Camphausen, M.A. Moses, W.D. Beecken, M.K. Khan, J. Folkman, M.S. O'Reilly, Radiation therapy to a primary tumor accelerates metastatic growth in mice, *Cancer Res.* 61 (5) (2001) 2207–2211.
- [32] O. Skaff, K.A. Jolliffe, C.A. Hutton, Synthesis of the side chain cross-linked tyrosine oligomers dityrosine, trityrosine, and pulcherosine, *J. Org. Chem.* 70 (2005) 7353–7363.
- [33] T. Chen, H. Xiong, J.F. Yang, X.L. Zhu, R.Y. Qu, G.F. Yang, Diaryl ether: a privileged scaffold for drug and agrochemical discovery, *J. Agric. Food Chem.* 68 (2020) 9839–9877.
- [34] Y. Xie, Z. Xu, P. Hu, X.T. Tian, Y.H. Lu, H.D. Jiang, C.G. Huang, Z.C. Shang, Synthesis of the isodityrosine moiety of seongsanamide A–D and its derivatives, *Mar. Drugs* 21 (7) (2023) 373.
- [35] X. Liu, F. Yun, L. Shi, Z.H. Li, N.R. Luo, Y.F. Jia, Roles of signaling pathways in the epithelial-mesenchymal transition in cancer, *Asian Pac. J. Cancer Prev.* 16 (15) (2015) 6201–6206.
- [36] M.Z. Kamran, P. Patil, R.P. Gude, Role of STAT3 in cancer metastasis and translational advances, *BioMed Res. Int.* 2013 (2013), 421821.